

ORIGINAL ARTICLE

A Systems Pharmacology Model of Erythropoiesis in Mice Induced by Small Molecule Inhibitor of Prolyl Hydroxylase Enzymes

I Singh¹, EE Nagiec², JM Thompson³, W Krzyzanski¹ and P Singh^{4*}

Mammalian erythropoiesis is a conserved process tightly controlled by the hypoxia-inducible factor (HIF1) pathway. In this study, a small molecule inhibitor (PHI-1) of prolyl-hydroxylase-2 (PHD2) enzyme involved in regulating HIF1 α levels was orally administered to male BALB/c mice at 10 and 30 mg/kg. A systems pharmacology model was developed based on the measured PHI-1 plasma exposures, kidney HIF1 α , kidney erythropoietin (EPO) mRNA, plasma EPO, reticulocyte counts, red blood cells, and hemoglobin levels. The model fit resulted in the estimation of drug potency (IC₅₀: 1.7 μ M), and systems parameters such as EPO mRNA turnover ($k_{deg_EPOmRNA}$: 0.43 hr⁻¹) and mean lifespan of reticulocytes (T_r : 81 hours). The model correctly described the observed 30–40-fold increase in kidney HIF1 α protein, ~1,000 fold increase in EPO mRNA and 2–3-fold increase in the reticulocytes at 30 mg/kg. This study presents the first parsimonious systems model of erythropoiesis to quantitatively describe the *in vivo* effects of PHD2 inhibition.

CPT Pharmacometrics Syst. Pharmacol. (2015) 4, e12; doi:10.1002/psp4.12; published online on 00 Month 2015.

Erythropoiesis is a physiological process that regulates production of red blood cells (RBCs) in mammalian species. Abnormal regulation of erythropoiesis due to iron deficiency, hemolysis, or chronic diseases results in various manifestations of anemia. A broad range of erythropoiesis stimulating agents (ESAs) including epoetin-alpha, epoetin-beta, and darbapoetin are currently being used for anemia treatment, but recent studies¹ have raised significant safety concerns due to increased risk of death, blood-clotting, strokes, and heart attacks in patients treated with doses above the recommended levels. Moreover, currently approved ESAs need to be administered via subcutaneous injection or intravenous infusion, and often require intravenous iron supplementation. Given these concerns, there is a critical need for novel therapeutic agents with enhanced efficacy, higher safety, lower costs, and oral route of delivery.

In recent years, stimulation of erythropoiesis via inhibitors of prolyl hydroxylase enzyme 2 (PHD2) has emerged as a new paradigm for anemia treatment. Two oral inhibitors of PHD2 developed by Fibrogen (San Francisco, CA) (FG-2216 and FG-4592) were reported² to demonstrate positive proof of concept (POC) in anemic nondialysis patients with chronic kidney disease (CKD). PHD2 regulates hydroxylation of HIF1 α ³ at two proline residues leading to degradation of HIF1 α via the von Hippel–Lindau (VHL) protein of the E3 ubiquitin ligase complex.⁴ To catalyze this process, PHD2 enzyme uses oxygen and 2-oxoglutarate (2-OG) as cosubstrates, and iron and ascorbate as cofactors.^{5–7} Inhibition of PHD2 leads to greater stabilization and nuclear translocation of HIF1 α protein, subsequent DNA binding, and increased gene expression of HIF1 α controlled genes

such as erythropoietin (EPO). Enhanced expression of EPO leads to an increase in bone marrow progenitor cells, reticulocytes, RBCs, and hemoglobin (HGB)⁸ that further compensates for the deficiency of oxygen under hypoxic and anemic conditions.

Despite decades of clinical experience with recombinant ESAs and significant advances in nonpeptide-based therapies, a clear mechanistic understanding of the erythropoiesis process is still lacking. Similar to the recently developed systems pharmacology models of NO metabolome, bone mineral density, and GnRH receptor modulation,^{9–11} a thorough understanding of the erythropoiesis time course and inherent exposure–response relationships is needed. Even though several mathematical models have been developed to explore the specific behavior of HIF1 α and its role in oxygen sensing and adaptation to hypoxia,¹² these modeling efforts have primarily focused on *in vitro* systems on short time scales, and do not account for multiscale dynamic processes linking HIF1 α activation in tissues to RBC production and HGB increase in circulation.

The goal of this study was to develop a parsimonious systems model to quantitatively describe the time course of erythropoiesis in mice. The proposed systems pharmacology model of erythropoiesis process is presented in **Figure 1**. Towards model development, a novel oral inhibitor of PHD2 developed at Pfizer Corporation (Cambridge, MA), henceforth referred to as PHI-1, was utilized to obtain the time-course data on relevant pharmacokinetic-pharmacodynamic (PK-PD) endpoints at time scales ranging from hours to weeks. A systems approach based on transduction compartments was utilized to integrate intracellular HIF1 α and EPO

¹Department of Pharmaceutical Sciences, School of Pharmacy and Pharmaceutical Sciences, University at Buffalo, Buffalo, New York, USA; ²Exploratory Drug Safety, Drug Safety Research and Development (DSRD), Pfizer, Cambridge, Massachusetts, USA; ³Inflammation Biology, Pfizer, Chesterfield, Missouri, USA; ⁴Pharmacokinetics-Dynamics and Metabolism (PDM), Pfizer, Cambridge, Massachusetts, USA; Current affiliation for I Singh: Clinical Pharmacology, Modeling and Simulation, Amgen, Thousand Oaks, California, USA. *Correspondence: P Singh (pratap.singh@pfizer.com)

Received 16 June 2014; accepted 7 October 2014; published online on 0 Month 2015. doi:10.1002/psp4.12

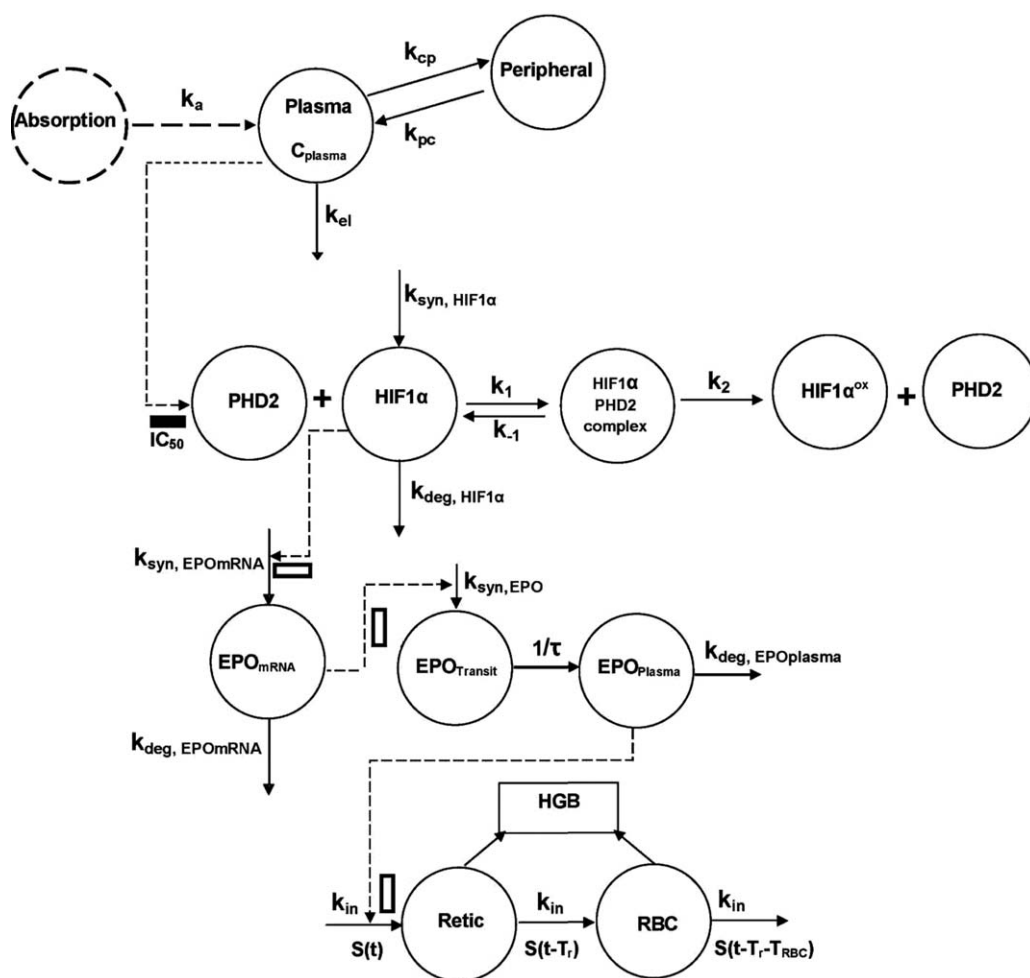


Figure 1 The proposed systems pharmacology model of erythropoiesis. Symbols and model operations are explained in the Methods section.

mRNA responses with downstream biomarkers such as EPO plasma levels, reticulocyte counts, RBC, and HGB. Predictive power of the systems model was tested by simulating RBC and HGB time profiles. The model was also used to simulate the time course of unobserved endpoints such as PHD2 activity profile in kidneys postdose administration.

RESULTS

Drug concentrations in plasma

Based on visual interpretation of drug absorption and distribution phases, a two-compartment PK model was selected to fit the drug plasma exposures (**Figure 2**). Subsequently, the estimated PK parameters were held constant to perform data fitting of the pharmacological responses. The data were simultaneously fitted for both doses to estimate PK parameters (**Table 1**). As shown in **Figure 2**, the PK profiles of two doses could be well described by the dose-dependent volume of distribution ($V1/F = 9.15L$, $V2/F = 2.4L$). The inset figure shows model fitting for drug absorption and distribution phase up to 2 hours after drug administration.

Kidney HIF1 α protein

The available experimental data suggest that the inhibition of PHD2 enzyme by PHI-1 results in reduction of HIF1 α hydroxylation, causing lower degradation and accumulation of HIF1 α protein in mice kidney cells (**Figure 3a**). We observed ~ 30 – 40 -fold increase in HIF1 α concentration in kidney tissues within 2–4 hours and return to its baseline between 12–24 hours after PHI-1 dosing. The observed HIF1 α data were fitted to the model (**Figure 1**) and relevant systems parameters were estimated (**Table 1**). The half maximal inhibitory concentration (IC_{50} , PHI-1) is estimated to be 1.7 μM . The estimated rate of HIF1 α synthesis ($k_{\text{syn, HIF1}\alpha}$) is 3,473 $AUhr^{-1}$. The plasma concentration of drug in this study was maintained above IC_{50} for ~ 5 hours at the 30 mg/kg dose.

Kidney EPO mRNA and plasma EPO protein

Following the accumulation of HIF1 α inside kidney cells, gene transcription processes are induced, leading to the expression of a wide range of proteins. At the 30 mg/kg dose, we observed $\sim 1,000$ -fold increase in EPO mRNA and plasma EPO protein, as shown in **Figure 3b,c**. The

Table 1 Estimates and coefficients of variation of model parameters

| Parameters | Estimated values | CV% |
|--------------------------------------|------------------------------|-----|
| <i>Pharmacokinetics</i> | | |
| k_a (hr^{-1}) | 8.5 | 54 |
| k_{el} (hr^{-1}) | 0.66 | 9 |
| k_{cp} (hr^{-1}) | 0.014 | 31 |
| k_{pc} (hr^{-1}) | 0.005 | 31 |
| V_1/F (L) | 9.15 | 35 |
| V_2/F (L) | 2.4 | 20 |
| $HIF1\alpha$ | | |
| $K_E \times PHD2_{tot0}$ | 9.9 | 14 |
| IC_{50} (μM) | 1.7 | 6 |
| γ_1 | 2.3 | 11 |
| $k_{deg,HIF1\alpha}$ (hr^{-1}) | 0 (fixed) | – |
| $HIF1\alpha$ (AU) | 351 | 7 |
| <i>EPO mRNA and Plasma EPO</i> | | |
| $k_{deg, EPO mRNA}$ (hr^{-1}) | 0.43 | 15 |
| τ (hr) | 2.7 | 7 |
| EPO_{mRNA0} | 0.8 | 13 |
| $EPO_{Plasma0}$ (ng/mL) | 0.047 | 4 |
| γ_2 | 2.8 | 5 |
| <i>Reticulocytes</i> | | |
| $Retic_0$ (% RBC) | 4.6 | 4 |
| T_r (hr) | 81 | 4 |
| SL | 0.2 | 18 |
| $MCH_{average}$ (g/cell) | 16×10^{-12} (fixed) | |
| <i>Secondary parameters</i> | | |
| $k_{syn,HIF1\alpha}$ (AU hr^{-1}) | 3473 | 13 |
| $k_{syn,EPO mRNA}$ (hr^{-1}) | 0.35 | 20 |
| $k_{syn, EPO}$ (ng/mL.hr) | 0.02 | 14 |
| $k_{deg, EPO Plasma}$ (hr^{-1}) | 0.37 | 7 |
| k_{in} (%cells hr^{-1}) | 0.05 | 7 |

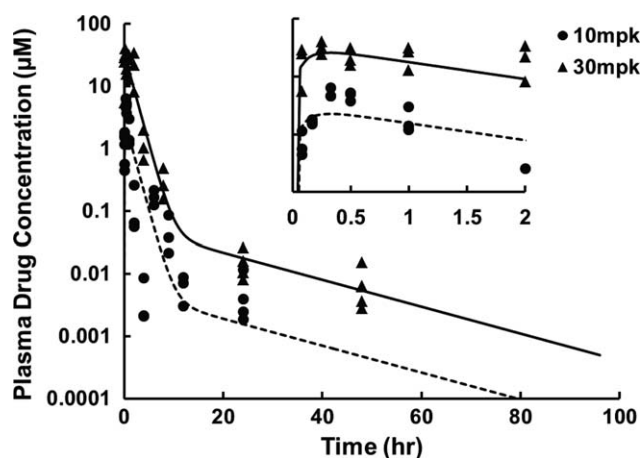


Figure 2 Pharmacokinetics (PK) of prolyl hydroxylase inhibitor PHI-1. The drug was given orally at two single doses of 10 (●) and 30 (▲) mg/kg to male BALB/C mice ($n = 3-6$, per time-point). The blood plasma samples were collected up to 96 hours. Symbols are experimentally observed plasma drug concentrations and lines (—, - -) are individually fitted PK curves for two doses. The inset figure shows model fitting in an earlier phase of drug absorption and drug distribution after 2 hours of drug administration. The estimated PK parameters are listed in **Table 1**.

EPO mRNA levels attain their peak expression level around 3–6 hours after drug administration, which is delayed from HIF1 α peaks by 2–4 hours. Plasma EPO concentrations attain a maximum between 6–12 hours after drug administration. At 10 mg/kg dose, the change was minimal for EPO mRNA and plasma EPO.

EPO mRNA and plasma EPO levels were fitted simultaneously for both doses. The estimated rate of degradation of EPO mRNA ($k_{deg, EPO mRNA}$) and plasma EPO protein ($k_{deg, EPO plasma}$) were 0.43 hr^{-1} and 0.374 hr^{-1} respectively. The delay between observed peaks for HIF1 α and EPO mRNA was well described by the model. The stimulation of EPO mRNA synthesis rate with the power function (estimated $\gamma_2 = 2.8$) fits the data well. Also, the delay in conversion of EPO mRNA to protein due to translational processes was well described by a single transit compartment with the mean transit time τ of 2.7 hours.

Reticulocytes

At a 30 mg/kg dose, the observed ~1,000-fold increase in EPO plasma concentration leads to a 3–4 fold increase in reticulocytes (**Figure 3d**). This observation is consistent with previously reported findings.¹³ To fit reticulocyte response, we assumed that EPO stimulates the synthesis rate of reticulocytes by a linear slope function of EPO plasma concentration. A cell lifespan¹⁴ based model was applied to capture the response profile by introducing only a single average reticulocyte lifespan time (T_r) which represents cell residence time in circulation. The estimated baseline reticulocyte ($Retic_0$) was 4.6% of RBC. The T_r was estimated to be 81 hours in mice, a value slightly higher than a T_r of 72.3 hours¹⁵ reported for rats treated with recombinant human erythropoietin. Another report¹⁶ suggests rhEPO causing ~2-fold increase in mice reticulocytes between 48–72 hours.

Simulation of RBC and HGB time profile

To test the predictive power of our systems model, we compared simulated RBC and HGB time profiles by overlaying them on experimentally obtained data points. Both RBC and HGB (**Figure 4a,b**) time profiles were well described. At the 10 mg/kg dose, there were no significant changes in observed RBC and HGB levels, consistent with the observed reticulocytes data. At the 30 mg/kg dose, the model simulation of the RBC time profile shows an increase in RBC levels from baseline due to an increase in reticulocytes that are released into circulation. RBC level starts to decline after life span of reticulocytes (T_r , 81 hours), and remain at plateau due to maturation of reticulocytes to mature RBCs. Since we assumed an RBC lifespan (T_{RBC}) of 24 days, RBC levels remain at their plateau during a 10-day simulation period. A similar profile was also observed in HGB levels. Our model predictions are consistent with other clinical data where HGB shows a proportional increase with RBC.¹⁷

Simulation of PHD2 activity time course

In order to predict the degree of PHD2 inhibition required to modulate downstream pharmacological responses, the time course of PHD2 activity post 10 and 30 mg/kg doses were simulated (**Figure 4c**). Since baseline PHD2 concentrations were not measured experimentally, simulated plots are presented as the ratio of active PHD2 concentration to the

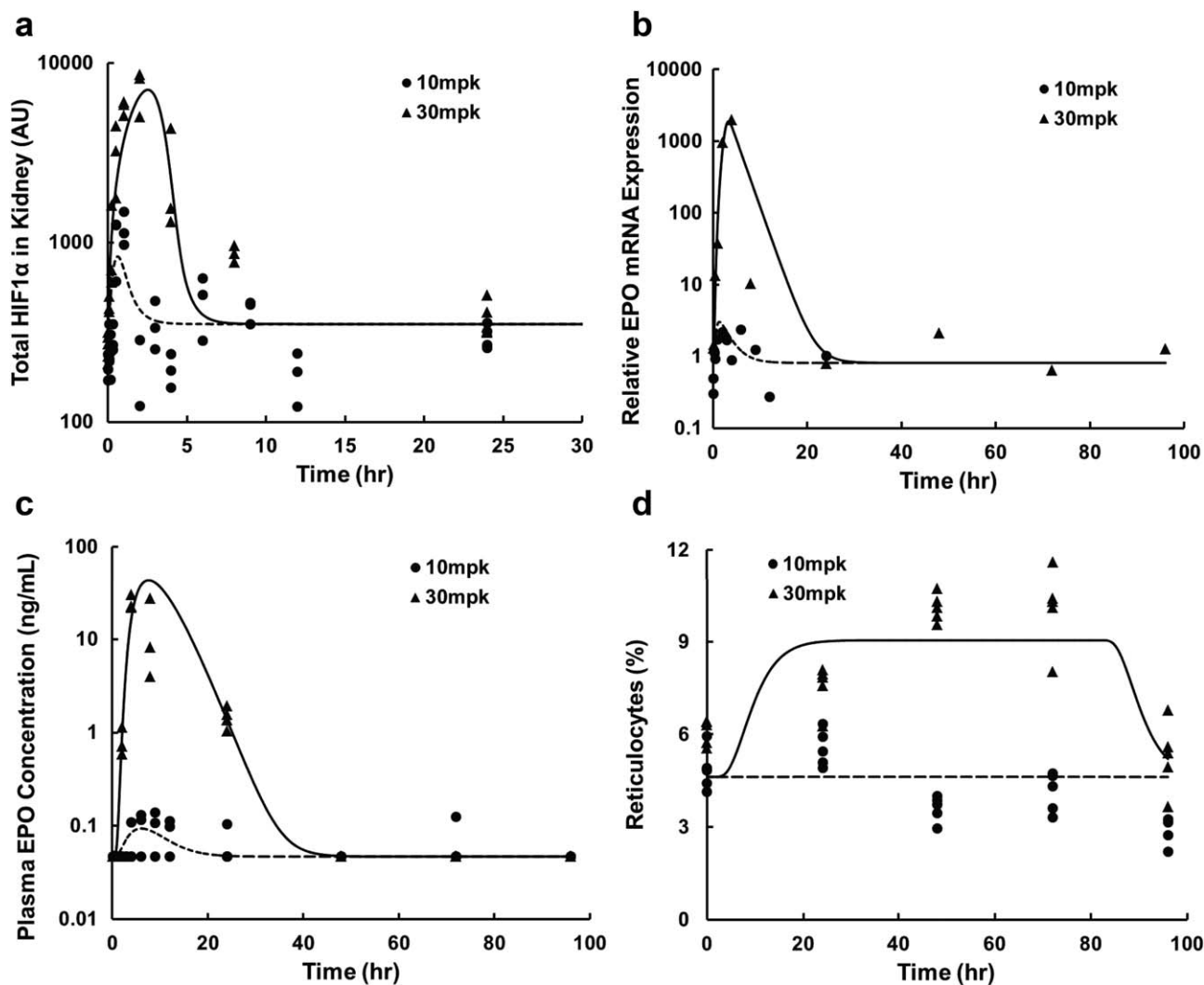


Figure 3 Pharmacological responses after single oral dose of 10 (●) and 30 (▲) mg/kg. (a) Total HIF1 α protein concentration from mice kidney. Symbols indicate naïve pooled experimental data and lines (---, —) are model predictions after simultaneous fitting two doses. Each measurement is presented in absorbance units (AU). (b) Kidney erythropoietin mRNA. Symbols indicate averaged experimental data, whereas lines (---, —) are model predictions. mRNA measurements at various timepoints are scaled relative to baseline at $t = 0$ before drug administration. (c) Plasma EPO protein concentrations in ng/mL. Symbols indicate naïve pooled experimental data whereas lines (---, —) are model predictions. (d) Reticulocytes measured as percentage of red blood cells (RBCs). Symbols indicate naïve pooled experimental data and lines (---, —) are model predictions after simultaneous fitting of two doses. The relevant parameters are listed in **Table 1**.

baseline PHD2 concentration. As shown in **Figure 4c**, at the 30 mg/kg dose, the model predicted a rapid decline of PHD2 activity from baseline (ratio = 1, 0% inhibition) to no PHD2 activity within 2 hours (ratio ~ 0 , 100% inhibition). Subsequently, $>50\%$ inhibition (ratio <0.5) is still seen up to 5 hours postdose. The active enzyme levels returned to baseline (ratio = 1) 8 hours post 30 mg/kg dose. In contrast, the peak inhibition of $<60\%$ (ratio >0.4) is predicted at 10 mg/kg with fast return to baseline within 4 hours postdose.

Simulation of PHI-1 dosing regimen to predict erythropoietic responses

We performed model-based simulations to predict erythropoietic responses in mice under various dosing regimens of PHI-1. Drug PK, reticulocytes, RBC, and HGB time profiles

were simulated after multiple doses of 10 and 30 mg/kg administered either every day (QD), every 2 days (Q2D), or every 3 days (Q3D), as shown in **Figures 5** and **6**. Based on model predictions, the 10 mg/kg dose may not be effective when administered QD over a period of 1 week in mice. Reticulocytes, RBC, and HGB did not show any increase at 10 mg/kg for any of the three regimens simulated, as shown in **Figure 5**. This is due to the limited drug exposure, where drug concentration remains below IC_{50} ($=1.7 \mu\text{M}$) value for most of the time. For 30 mg/kg dosing, the model predicts sustained erythropoietic response for all three regimens. In the case of the 30 mg/kg QD dose, reticulocyte levels increased by ~ 4 -fold, resulting in $\sim 30\%$ increase in RBC levels (plateau) and >4 g/dL increase in HGB levels (plateau), as shown in **Figure 6**.

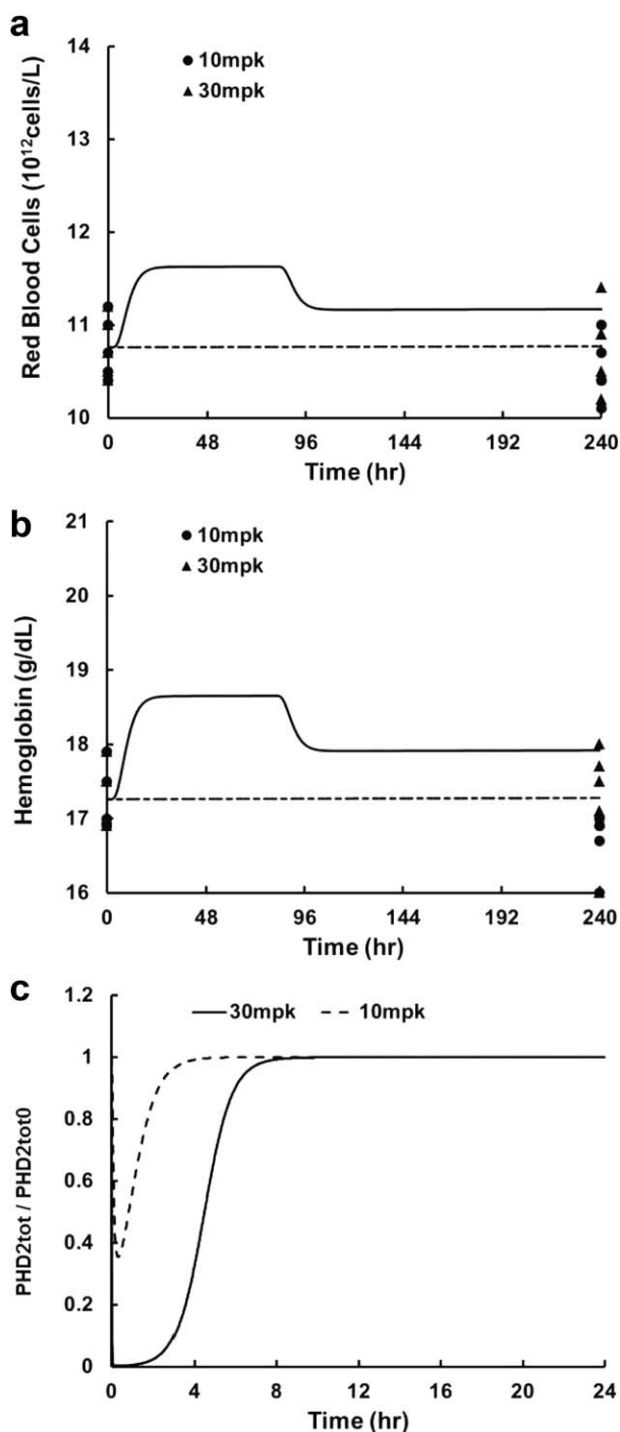


Figure 4 Simulation for red blood cells, hemoglobin and PHD2 time profiles. (a) Simulated and observed red blood cells time profile for 10 (●) and 30 (▲) mg/kg dose. (b) Simulated and observed hemoglobin time profiles for 10 (●) and 30 (▲) mg/kg dose. Lines (---, —) are model simulation for two doses. (c) Total PHD2 activity time course simulated for two doses of 10 (---) and 30 (—) mg/kg. The plots are presented as the ratio of total active PHD2 concentration and baseline PHD2 (PHD2tot₀) concentration.

DISCUSSION

This study presents a comprehensive analysis of the erythropoietic responses to oral administration of PHI-1 in mice. The systems pharmacology model reported in this study was built by incorporating all major components of the PHD2-HIF1 α pathway that control the erythropoietic response, enabling us to perturb the system with various stimuli at different component levels. Unlike traditional systems models that borrow parameters from the literature, the availability of rich experimental data enabled us to estimate most of the systems parameters. Data collection at both the plasma and tissue level allowed us to build a multiscale model with transduction compartments to vertically integrate the intracellular HIF1 α and EPO mRNA responses in kidney with *in vivo* markers of erythropoiesis such as EPO plasma levels and reticulocyte counts.

A two-compartment model was applied to describe the drug PK at 10 and 30 mg/kg. The nonlinearity in PK could be well described by estimating two dose-dependent volumes of distribution ($V1/F$ and $V2/F$). For simulation of the multiple dosing scenarios in **Figures 5** and **6**, the assumption of linearity within each dose group was applied to predict PK and other PD marker profiles. Based on the mechanism of drug action a direct effect model¹⁸ was chosen to explain inhibition of PHD2 by PHI-1. The drug IC_{50} was estimated to be 1.7 μ M, whereas the *in vitro* IC_{50} in the HIF1 α functional luciferase assay (unpublished data) was 5.65–10 μ M. Given the physiological difference between *in vitro* cells and *in vivo* systems, this 3–6-fold difference is not surprising. It can be observed that drug in plasma remains above its estimated IC_{50} value of 1.7 μ M for ~5 hours at the 30 mg/kg dose (**Figure 2**). Although there was no direct measurement of PHD2 activity postdosing, the model predictions for 30 mg/kg indicate significant enzyme inhibition up to 5 hours (<50% active enzyme) with return to baseline only after 8 hours (**Figure 4c**). Consistent with the minimal PD response, the 10 mg/kg dose resulted in weak PHD2 inhibition, with a return to baseline within 4 hours and maximum inhibition of <60% (**Figure 4c**).

Following the enzymatic mechanism of PHD2-mediated hydroxylation of HIF1 α , our proposed model incorporates equations with hybrid parameters to explain the pharmacodynamic behavior of HIF1 α . The primary parameter listed in **Table 1** as $k_E PHD2_0$ ($k_E \times PHD2_0$) is a hybrid parameter that includes reaction rate constants and baseline PHD2 concentration. Since individual rate constants are difficult to estimate and baseline PHD2 concentrations were not measured, this new parameter is estimated in our model fitting. Plasma EPO profiles were well described by our model, and peak concentrations were captured at both doses. In a typical indirect response model,¹⁹ the baseline concentration of drug is assumed to be zero, but in case of EPO stimulation by HIF1 α , there is a nonzero baseline value of HIF1 α in the absence of drug administered. Since use of both SC_{50} and S_{max} resulted in imprecise parameters estimation, we incorporated a power function-based stimulation of EPO mRNA by HIF1 α with sigmoid factor γ_2 and a zero-order stimulation of EPO protein production by EPO mRNA. A single transit compartment could explain the

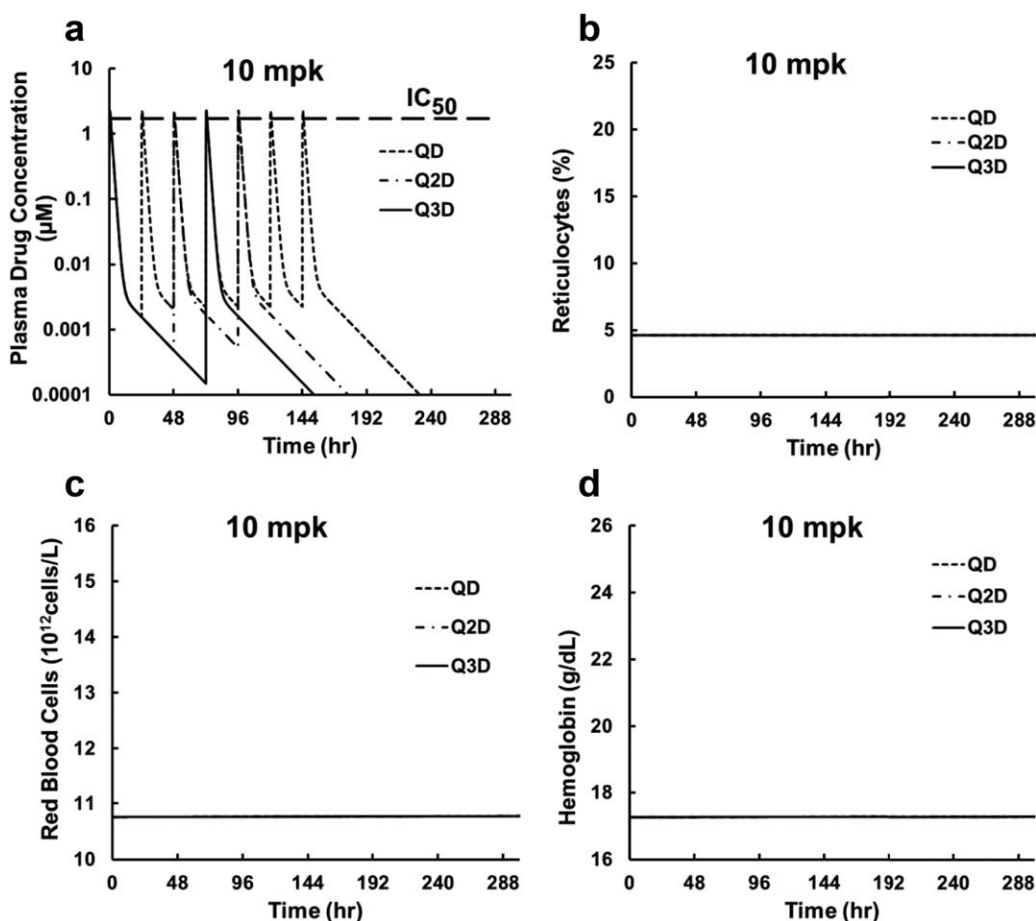


Figure 5 Simulation results for 10 mg/kg daily (QD), every other day (Q2D), and every third day (Q3D) dosing of PHI-1. (a) Drug plasma PK, (b) reticulocytes, (c) red blood cells, and (d) hemoglobin time course.

delay in peak levels of EPO mRNA and EPO in plasma. The predicted half-life of endogenous plasma EPO ($\ln 2 / k_{deg, EPO_{plasma}}$) is about 1.8 hours for mice, a value lower than that of rHuEPO (epoetin alpha) in rats ($t_{1/2} = 2.5$ hours) and dogs ($t_{1/2} = 7.2$ hours) as published elsewhere.²⁰ This difference may be due to the body weight-dependent drug clearance.²¹ Also, there might be differences in the level of EPO receptor population and binding kinetics across species.

The stimulation of reticulocytes by plasma EPO was modeled by a cell lifespan model suggested by Krzyzanski *et al.*¹⁴ Reticulocytes stimulation due to EPO was modeled as slope function SL. The estimated reticulocyte lifespan in the circulation $Tr = 81$ hours is longer than the reticulocyte maturation time under baseline condition reported as 20–40 hours for mouse.²² This may be consistent with stress erythropoiesis due to erythropoietin stimulation where the circulating reticulocyte lifespan increases because of a release of immature reticulocytes from the bone marrow.²³ An increase in estimates of Tr for stress reticulocytes has been also reported for rats¹⁵ and humans.²⁴

To further test the versatility of our proposed model we performed simulations to get profiles of unknown PHD2 concentration and for known RBCs and HGB after a sin-

gle dose of 10 mg/kg or 30 mg/kg. Further, the model was applied to predict RBC and HGB modulation after multiple doses of PHI-1 administered daily, every 2nd day or every 3rd day (Figures 5 and 6). These predictions provide valuable insights into drug dose and frequency that is tailored to achieve a certain level of HGB increase based on the anemia patient's baseline levels. Although the current model is developed for mice, it can easily be applied to virtually any animal model and for humans, since most mammals follow the canonical PHD2-HIF1 α based pathway for erythropoietic stimulation. Application of allometric scaling²¹ on various model parameters should provide reasonable simulated HGB profiles in human as well.

In conclusion, the model proposed in this study incorporates a systems pharmacology-based approach to illustrate murine erythropoiesis. To our knowledge, this is the first report of a mechanism based model to explain PHD inhibitor's effect on erythropoietic response. Overall, our model fits the experimental data very well across all the PD markers measured in this study. In spite of PD measurements with large variability, model parameters could be estimated with reasonable precision. Although the current model is developed using single-dose administration in

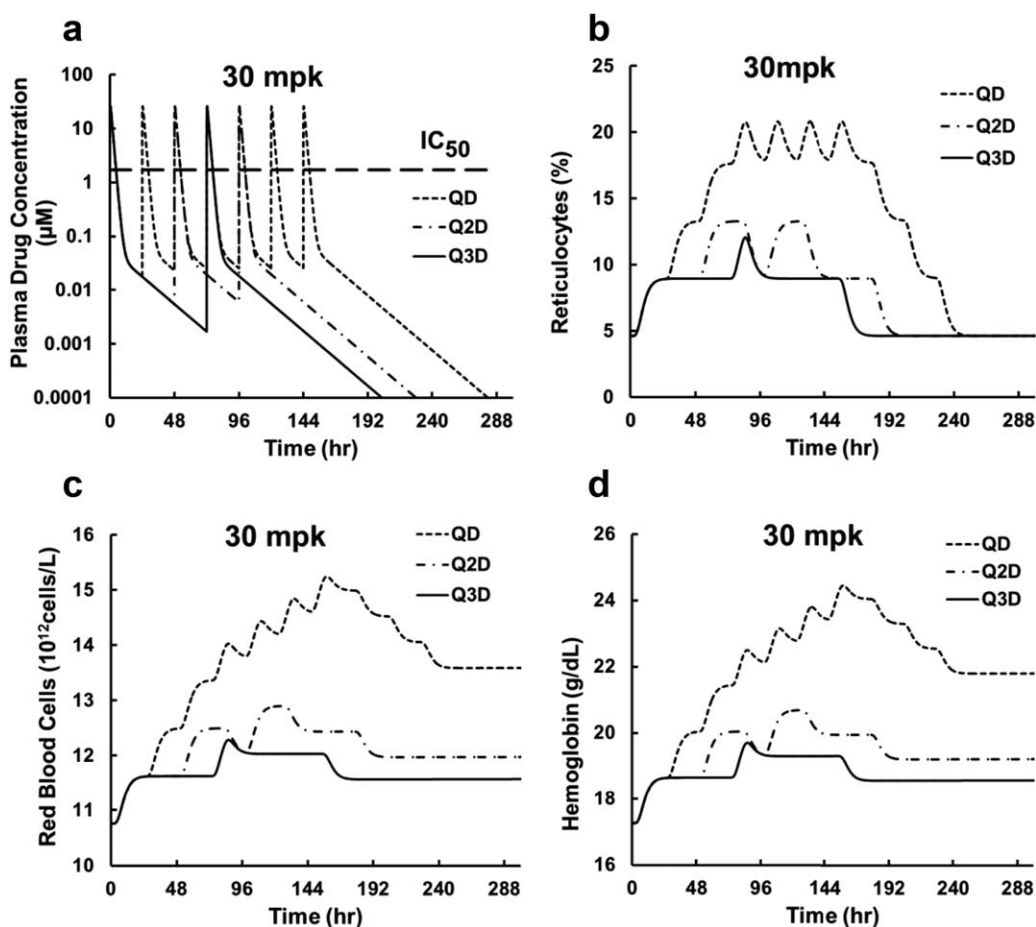


Figure 6 Simulation results for 30 mg/kg daily (QD), every other day (Q2D), and every third day (Q3D) dosing of PHI-1. (A) Drug plasma PK, (b) reticulocytes, (c) red blood cells, and (d) hemoglobin time course.

mice, we showcase its application in predicting erythropoietic responses in multiple dosing scenarios within reasonable assumptions. The current model can further be improved by incorporating more data from future studies. Application of current model with further extension can help guide future preclinical study designs and human dose predictions.

METHODS

Experimental design

Male BALB/c mice were randomly grouped before oral administration of vehicle (0.5% methylcellulose with 0.025% Tween 20) or compound (0.2 ml). Inhibitor compound PHI-1 was dosed at 10 and 30 mg/kg orally. Subsets of mice were euthanized with CO_2 inhalation before terminal bleed via cardiac stick at the appropriate time-point (0.25–96 hours). Blood was collected into microtainer collection tubes with EDTA. Kidney and liver tissue was collected immediately after bleeds and flash-frozen in liquid nitrogen. Tissue and plasma samples were stored at -80°C . Plasma was used for PK and EPO analysis. HIF1 α and EPO mRNA were extracted from kidney samples. Whole blood was used for percent reticulocyte,

RBC, and HGB analysis. Details of the experimental design and sample analysis are provided in the **Supplementary Material**.

Systems pharmacology model

Plasma drug concentration. The current study includes single oral dose administration of prolyl hydroxylase inhibitor PHI-1 at 10 and 30 mg/kg. A two-compartment model with central and peripheral compartments was selected as our final PK model. Drug absorption was modeled by first-order absorption rate constant (k_a). The peripheral compartment is connected with central compartment via reversible first-order rate constants (k_{cp} , k_{pc}), and the elimination from the central compartment is also assumed to be first-order rate constant (k_e). Two different volumes of distribution ($V1/F$, $V2/F$) were estimated for 10 and 30 mg/kg doses.

Here, F denotes the oral drug bioavailability. The output fitted variable is the drug plasma concentration C_{plasma} .

Pharmacological response. A systems biology-based approach was applied to explain the drug mechanism of action. Stepwise model development is explained below with relevant model equations for each observed PD marker.

PHD2-HIF1 α interaction. PHD2 enzyme deactivation due to PHI-1 binding is described by an inhibitory direct effect model.

$$\text{PHD2}_{\text{tot}} = \text{PHD2}_{\text{tot}_0} \times \left(1 - \frac{C_{\text{plasma}}^{\gamma_1}}{IC_{50}^{\gamma_1} + C_{\text{plasma}}^{\gamma_1}}\right) \quad (1)$$

Here, $\text{PHD2}_{\text{tot}_0}$ is the baseline concentration of total active PHD2 enzymes in the absence of drug; PHD2_{tot} is the total active PHD2 enzyme postdosing; IC_{50} is the drug plasma concentration to achieve 50% decrease in PHD2 concentration. The hydroxylation of HIF1 α by PHD2 is described by an enzyme-based reaction model.



PHD2 binding to HIF1 α results in an unstable complex formation and after hydroxylation of HIF1 α , PHD2 is released back from the complex. Following is the mathematical equation for this reaction kinetics to describe HIF1 α turnover (see **Supplementary Material** for details):

$$\frac{d(\text{HIF1}\alpha)}{dt} = k_{\text{syn,HIF1}\alpha} - \left(k_{\text{deg,HIF1}\alpha} + k_E \times \text{PHD2}_{\text{tot}_0} \times \left(1 - \frac{C_{\text{plasma}}^{\gamma_1}}{IC_{50}^{\gamma_1} + C_{\text{plasma}}^{\gamma_1}}\right) \right) \times \text{HIF1}\alpha \quad (3)$$

Initial condition:

$$\text{HIF1}\alpha(0) = \text{HIF1}\alpha_0 \quad (4)$$

HIF1 α_0 is the baseline HIF1 α level. In the absence of drug, degradation of HIF1 α due to PHD2-mediated hydroxylation is the most dominating pathway contributing to its natural rate of degradation, so for fitting purposes the contribution of the basal HIF1 α protein degradation process (independent of PHD2 driven degradation) is ignored and $k_{\text{deg,HIF1}\alpha}$ is fixed to 0.

Kidney EPO mRNA and plasma EPO. The accumulation of HIF1 α results in transcription of EPO genes. Stimulation of EPO mRNA followed by translational processes results in EPO protein synthesis and further release into plasma. To capture this in our model we assumed a power function (γ_2) based stimulation of EPO mRNA synthesis rate ($k_{\text{syn,EPO mRNA}}$) by HIF1 α with first order EPO mRNA degradation rate $k_{\text{deg,EPO}}$. Delay between EPO mRNA to EPO protein translation and secretion to plasma was modeled by a signal transduction model²⁵ with one transit compartment of mean transit time τ . The plasma EPO synthesis rate was assumed to be proportional to the EPO mRNA levels. Baseline EPO synthesis rate $k_{\text{syn,EPO}}$ was assumed to be zero-order rate constant and the degradation rate $k_{\text{deg,EPO plasma}}$, a first-order rate constant. Equations describing these processes are listed below:

$$\frac{d(\text{EPO}_{\text{mRNA}})}{dt} = k_{\text{syn,EPO mRNA}} \times \left[\frac{\text{HIF1}\alpha}{\text{HIF1}\alpha_0} \right]^{\gamma_2} - k_{\text{deg,EPO mRNA}} \times \text{EPO}_{\text{mRNA}} \quad (5)$$

$$\frac{d(\text{EPO}_{\text{transit}})}{dt} = k_{\text{syn,EPO}} \times \text{EPO}_{\text{mRNA}} - \frac{1}{\tau} \times \text{EPO}_{\text{transit}} \quad (6)$$

$$\frac{d(\text{EPO}_{\text{plasma}})}{dt} = \frac{1}{\tau} \times \text{EPO}_{\text{transit}} - k_{\text{deg,EPO plasma}} \times \text{EPO}_{\text{plasma}} \quad (7)$$

The initial conditions for differential equations were determined by the baseline (steady state) values:

$$\text{EPO}_{\text{mRNA}}(0) = \text{EPO}_{\text{mRNA}_0} \quad (8)$$

$$\text{EPO}_{\text{Transit}}(0) = \text{EPO}_{\text{Transit}_0} \quad (9)$$

$$\text{EPO}_{\text{Plasma}}(0) = \text{EPO}_{\text{Plasma}_0} \quad (10)$$

For simplicity, it is assumed that $k_{\text{deg,EPO plasma}} = 1/\tau$. Baseline equations to solve above-mentioned differential equations are listed below:

$$k_{\text{syn,EPO mRNA}} = k_{\text{deg,EPO mRNA}} \times \text{EPO}_{\text{mRNA}_0} \quad (11)$$

$$k_{\text{syn,EPO}} = 1/\tau \times \frac{\text{EPO}_{\text{Plasma}_0}}{\text{EPO}_{\text{mRNA}_0}} \quad (12)$$

$$\text{EPO}_{\text{Transit}_0} = \text{EPO}_{\text{Plasma}_0} \quad (13)$$

Stimulation of reticulocytes. An increase in plasma EPO protein concentration stimulates progenitor cells in bone marrow that results in an increase in reticulocytes and RBCs in blood. EPO stimulates the proliferation and differentiation of erythroid progenitors into erythrocytes. Binding of EPO to its receptors on erythroid cells affects the stimulation process at different stages of cell differentiation. In the absence of data availability from each stage of erythroid cells differentiation, we present a model where only reticulocytes data are described. This model is adopted from a previously published cell lifespan model.¹⁴ According to this model, each reticulocyte spends the same time T_r (lifespan of reticulocytes) in circulation and converts to a mature erythrocyte. EPO stimulates the release rate of reticulocytes from bone marrow to plasma (k_{in}). Since reticulocytes were measured in blood, T_r is the mean residence time of reticulocytes in the circulation. Stimulation of reticulocytes production ($S(t)$) by EPO is modeled as a slope function.

$$\frac{d(\text{Retic})}{dt} = k_{in} \times S(t) - k_{in} \times S(t - T_r) \quad (14)$$

Where, $S(t) = \left(1 + SL \times \text{EPO}_{\text{plasma}}(t)\right)$

Prior to the drug treatment, baseline reticulocytes are defined as:

$$\text{Retic}(0) = \text{Retic}_0 \quad (15)$$

Following the steady state solution:

$$\text{Retic}_0 = k_{in} \times T_r \times (1 + SL \times \text{EPO}_{\text{plasma}_0}) \quad (16)$$

Model simulation

For model validation purposes, we performed simulations for RBC and HGB time profiles. The estimated parameters

were kept constant for model simulations. Application of a systems pharmacology-based approach enabled us to predict unknown biomarker profiles such as kidney PHD2 concentration levels and erythropoietic responses under various dosing scenarios.

Simulation of RBC and HGB time profile. RBC and HGB concentrations were measured on day 0 (predose) and day 10 for the 10 and 30 mg/kg doses. Therefore, simulations were performed for two doses (10 mg/kg and 30 mg/kg) and simulated time profiles were overlaid on experimentally observed data. The mice RBC lifespan (T_{RBC}) was assumed to be 24 days.^{26,27} The maturation rate for the reticulocytes is the production rate for mature RBC_M. Analogous to reticulocytes, we applied the lifespan model to simulate the RBC_M time course.

Similar to Eq. 14 for reticulocytes, the equation for RBC_M can be written as follows:

$$\frac{d(RBC_M)}{dt} = N_{k_{in}} \times S(t - T_r) - N_{k_{in}} \times S(t - T_r - T_{RBC}) \quad (17)$$

To predict absolute cell numbers, k_{in} is converted to $N_{k_{in}}$ (Eq. S1). The final simulated output is presented as:

$$RBC = Retic + RBC_M \quad (18)$$

The initial condition for Eq. 17 can be defined as:

$$RBC_M(0) = RBC(0) - Retic(0) \quad (19)$$

Since there was no statistically significant difference in MCH (mean corpuscular hemoglobin) values measured among all mice after various treatments, the average $MCH_{average}$ (Table 1) was calculated to simulate HGB time profile. HGB was calculated by linear equation:

$$HGB = MCH_{Average} \times RBC \quad (20)$$

Simulation of PHD2 time profile. As discussed above, an inhibitory direct effect model could describe active PHD2 enzyme removal (Eq. 1). Since data collection did not involve baseline PHD2 concentration (PHD2₀) measurements, simulation for both doses was performed to predict the ratio PHD2/PHD2₀.

Dosing regimen simulation. Various multiple dosing regimens were simulated to elicit the erythropoietic response at 10 and 30 mg/kg doses orally administered QD, Q2D, and Q3D over 1 week. Model-estimated parameters were used to simulate PK, reticulocytes, RBC, and HGB time profiles. PK was assumed to be linear within each multiple dosing regimen.

All model fittings and simulations were performed using ADAPT 5 software.²⁸

Acknowledgments. This study was supported by University at Buffalo-Pfizer Strategic Alliance and NIH Grant GM57980 from the National Institutes of General Medical Sciences.

Author Contributions. I. S., W. K., and P. S. wrote the article. P. S. designed the research. E. N. and J. M. performed the research. I. S. analyzed the data.

Conflict of Interest. The authors declare no conflict of interest.

Study Highlights

WHAT IS THE CURRENT KNOWLEDGE ON THIS TOPIC?

- ✓ There are many experimental data-based reports on PHI-1-induced erythropoiesis in the literature, but there is no systems pharmacology model describing the quantitative link between different erythropoietic responses.

WHAT QUESTION DID THIS STUDY ADDRESS?

- ✓ To develop a parsimonious systems model that is able to quantitatively describe the time course of the erythropoiesis process and apply a model-based approach in designing preclinical studies.

WHAT THIS STUDY ADDS TO OUR KNOWLEDGE

- ✓ We provide a mechanism-based systems model to explain PHI-1 effects on erythropoietic response.

HOW THIS MIGHT CHANGE CLINICAL PHARMACOLOGY AND THERAPEUTICS

- ✓ The current model provides support in assessing the impact of various dosing scenarios in preclinical studies that can help in optimal designing and reducing the number of studies. The model can also be translated to humans and in predicting human clinical doses.

1. Unger, E.F., Thompson, A.M., Blank, M.J. & Temple, R. Erythropoiesis-stimulating agents—time for a reevaluation. *N. Engl. J. Med.* **362**, 189–192 (2010).
2. Beuck, S., Schanzer, W. & Thevis, M. Hypoxia-inducible factor stabilizers and other small-molecule erythropoiesis-stimulating agents in current and preventive doping analysis. *Drug Test. Anal.* **4**, 830–845 (2012).
3. Dayan, F., Roux, D., Brahimi-Horn, M.C., Pouyssegur, J. & Mazure, N.M. The oxygen sensor factor-inhibiting hypoxia-inducible factor-1 controls expression of distinct genes through the bifunctional transcriptional character of hypoxia-inducible factor-1 α . *Cancer Res.* **66**, 3688–3698 (2006).
4. Maxwell, P.H. *et al.* The tumour suppressor protein VHL targets hypoxia-inducible factors for oxygen-dependent proteolysis. *Nature.* **399**, 271–275 (1999).
5. Bruick, R.K. & McKnight, S.L. A conserved family of prolyl-4-hydroxylases that modify HIF. *Science.* **294**, 1337–1340 (2001).
6. Jaakkola, P. *et al.* Targeting of HIF- α to the von Hippel-Lindau ubiquitylation complex by O₂-regulated prolyl hydroxylation. *Science.* **292**, 468–472 (2001).
7. Yu, F., White, S.B., Zhao, Q. & Lee, F.S. HIF-1 α binding to VHL is regulated by stimulus-sensitive proline hydroxylation. *Proc. Natl. Acad. Sci. USA.* **98**, 9630–9635 (2001).
8. Elliott, S., Pham, E. & Macdougall, I.C. Erythropoietins: a common mechanism of action. *Exp. Hematol.* **36**, 1573–1584 (2008).
9. Vega-Villa, K., Pluta, R., Lonser, R. & Woo, S. Quantitative systems pharmacology model of NO metabolome and methemoglobin following long-term infusion of sodium nitrite in humans. *CPT Pharmacometrics Syst. Pharmacol.* **2**, e60 (2013).
10. Peterson, M.C. & Riggs, M.M. Predicting nonlinear changes in bone mineral density over time using a multiscale systems pharmacology model. *CPT Pharmacometrics Syst. Pharmacol.* **1**, e14 (2012).
11. Riggs, M.M., Bennets, M., van der Graaf, P.H. & Martin, S.W. Integrated pharmacometrics and systems pharmacology model-based analyses to guide GnRH receptor

- modulator development for management of endometriosis. *CPT Pharmacometrics Syst. Pharmacol.* **1**, e11 (2012).
12. Qutub, A.A. & Popel, A.S. A computational model of intracellular oxygen sensing by hypoxia-inducible factor HIF1 alpha. *J. Cell. Sci.* **119**, 3467–3480 (2006).
 13. Hsieh, M.M. *et al.* HIF prolyl hydroxylase inhibition results in endogenous erythropoietin induction, erythrocytosis, and modest fetal hemoglobin expression in rhesus macaques. *Blood.* **110**, 2140–2147 (2007).
 14. Krzyzanski, W., Ramakrishnan, R. & Jusko, W.J. Basic pharmacodynamic models for agents that alter production of natural cells. *J. Pharmacokinet. Biopharm.* **27**, 467–489 (1999).
 15. Woo, S., Krzyzanski, W. & Jusko, W.J. Pharmacokinetic and pharmacodynamic modeling of recombinant human erythropoietin after intravenous and subcutaneous administration in rats. *J. Pharmacol. Exp. Ther.* **319**, 1297–1306 (2006).
 16. Bugelski P.J. *et al.* Pharmacodynamics of recombinant human erythropoietin in murine bone marrow. *Pharm. Res.* **25**, 369–378 (2008).
 17. Krzyzanski, W., Jusko, W.J., Wacholtz, M.C., Minton, N. & Cheung, W.K. Pharmacokinetic and pharmacodynamic modeling of recombinant human erythropoietin after multiple subcutaneous doses in healthy subjects. *Eur. J. Pharm. Sci.* **26**, 295–306 (2005).
 18. Sheiner, L.B., Stanski, D.R., Vozeh, S., Miller, R.D. & Ham, J. Simultaneous modeling of pharmacokinetics and pharmacodynamics: application to d-tubocurarine. *Clin. Pharmacol. Ther.* **25**, 358–371 (1979).
 19. Dayneka, N.L., Garg, V. & Jusko, W.J. Comparison of four basic models of indirect pharmacodynamic responses. *J. Pharmacokinet. Biopharm.* **21**, 457–478 (1993).
 20. Egrie, J.C., Dwyer, E., Browne, J.K., Hitz, A. & Lykos, M.A. Darbepoetin alfa has a longer circulating half-life and greater in vivo potency than recombinant human erythropoietin. *Exp. Hematol.* **31**, 290–299 (2003).
 21. Woo, S. & Jusko, W.J. Interspecies comparisons of pharmacokinetics and pharmacodynamics of recombinant human erythropoietin. *Drug Metab. Dispos.* **35**, 1672–1678 (2007).
 22. Koury, M.J., Koury, S.T., Kopsombut, P. & Bondurant, M.C. In vitro maturation of nascent reticulocytes to erythrocytes. *Blood.* **105**, 2168–2174 (2005).
 23. Wiczling, P., Ait-Oudhia, S. & Krzyzanski, W. Flow cytometric analysis of reticulocyte maturation after erythropoietin administration in rats. *Cytometry.* **75**, 584–592 (2009).
 24. Perez-Ruixo, J.J., Krzyzanski, W. & Hing, J. Pharmacodynamic analysis of recombinant human erythropoietin effect on reticulocyte production rate and age distribution in healthy subjects. *Clin. Pharmacokinet.* **47**, 399–415 (2008).
 25. Mager, D.E. & Jusko, W.J. Pharmacodynamic modeling of time-dependent transduction systems. *Clin. Pharmacol. Ther.* **70**, 210–216 (2001).
 26. Mouneimne, Y., Tosi, P.F., Barhoumi, R. & Nicolau, C. Electroinsertion of xeno proteins in red blood cell membranes yields a long lived protein carrier in circulation. *Biochim. Biophys. Acta.* **1066**, 83–89 (1991).
 27. Burwell, E.L., Brickley, B.A. & Finch, C.A. Erythrocyte life span in small animals: comparison of two methods employing radioiron. *Am. J. Physiol.* **172**, 718–724 (1953).
 28. D'Argenio, D.Z., Schumitzky, A. & Wang, X. ADAPT 5 User's Guide: Pharmacokinetic/Pharmacodynamic Systems Analysis Software 2009.

© 2015 The Authors *CPT: Pharmacometrics & Systems Pharmacology* published by Wiley Periodicals, Inc. on behalf of American Society for Clinical Pharmacology and Therapeutics. This is an open access article under the terms of the Creative Commons Attribution-NonCommercial License, which permits use, distribution and reproduction in any medium, provided the original work is properly cited and is not used for commercial purposes.

Supplementary information accompanies this paper on the *CPT: Pharmacometrics & Systems Pharmacology* website (<http://www.wileyonlinelibrary.com/psp4>)